

report of 5th semester project work

**Parameter Estimation for Quantitative Analysis
of the NF- κ B Signal Transduction Pathway
and a Further Induced Target Gene**

by
Achim Boltz

Institute of Pharmacy and Molecular Biotechnology IPMB,
University of Heidelberg, Germany

private adress: Fritz-Frey-Strasse 8, 69121 Heidelberg,

e-mail adress: satchmo2000@t-online.de

5th of may 2005

Contents

1	Introduction	3
2	Methods	6
2.1	Model, Variables and Parameters	6
2.2	(A) Lipniacki's parameters with optimized normalization factors	12
2.3	(B) Optimization of parameters with fixed normalization factors	12
2.4	(C) Optimization of both parameters and normalization factors	12
3	Results	13
3.1	Parameter estimation	13
3.2	(A) Lipniacki's parameters with optimized normalization factors	13
3.3	(B) Optimization of parameters with fixed normalization factors	14
3.4	(C) Optimization of both parameters and normalization factors	14
3.5	Comparison of model and measured data graphs	17
4	Conclusions and Outlook	18
4.1	Applications	19
5	Acknowledgements	21
	References	22
6	Appendix	23

Abstract

Measurements of several protein concentrations involved in the regulatory module of nuclear factor κ B (NF- κ B) are compared with a mathematical model including 15 factors of the NF- κ B signalling pathway (Lipniacki et al. 2004). The unknown parameters are estimated and optimized using a least squares fit with the optimization software tool MUSCOD-II. The NF- κ B regulatory proteins lie at the heart of most inflammatory responses and can also damage tissue and cause severe pain. In response to extracellular inducers like TNF or IL-1, the IKK kinase activates the I κ B kinase (IKK) by phosphorylation into its active form (IKKa), a form capable of phosphorylating I κ B α , leading to I κ B α degradation. Formerly in complex with I κ B α sequestered NF- κ B is set free and transported into the nucleus. It triggers transcription of its inhibitors A20 and I κ B α beneath numerous other genes. Newly synthesized I κ B α sequesters nuclear NF- κ B and leads it out of the nucleus, while A20 decreases the IKKa activity by converting it into an inactive form IKKi. The constructed model contains the two described negative feedback-loops and also integrates two-compartment kinetics in both cytoplasm and nucleus. It is modeled by means of 15 ordinary differential equations. All 40 parameters used in the model equations can be changed to minimize the discrepancy between the two graphs (of modeled and measured values) for each measurement point in time. At the same time, the normalization factors of all 11 measured factors are estimated and optimized. The validation of estimated parameters could allow to generate quantitative predictions for possible cell responses after stimulation or inhibition of involved regulatory factors like enzymes and mRNA as well as other known NF- κ B target genes and their products.

1 Introduction

The nuclear factor κ B (NF- κ B) regulates various genes involved in pathogene and cytokine inflammation, as well as in intercellular signalling during normal vertebrate development and cell proliferation. The inflammatory responses happen as a reaction to infections or injuries to help protecting cells from stress factors. But in excessive magnitude, they can also damage tissue and therefore cause severe pain as in rheumatic arthritis, for example. The NF- κ B family consists of five members termed NF- κ B1 (p50/p105), NF- κ B2 (p52/p100), RelA (p65),

RelB and c-Rel, which form a variety of homo- and heterodimers. The precursors p105 to NF- κ B1 and p100 to NF- κ B2 must be processed post-transcriptional to their active forms p50 and p52, respectively. Each dimer activates its own characteristic set of genes, but the ubiquitously expressed heterodimer NF- κ B1:RelA (p50:p65) shows the main inducible NF- κ B binding activity.

In resting cells, p50:p65 heterodimers (herein named NF- κ B) are sequestered in the cytoplasm by association with proteins of the I κ B family. It includes I κ B α , I κ B β , I κ B ϵ , I κ B γ and Bcl-3, beneath p105 and p100, which have homologous functions to I κ B, using their C-terminal ankyrin-repeat region to bind NF- κ B. But I κ B α plays the main role for inhibition of NF- κ B. Its synthesis is controlled by a highly NF- κ B-responsive promoter generating autoregulation of NF- κ B signaling.

In response to binding of diverse extracellular signal factors like TNF α or interleukin-1 (IL-1) and not fully understood to viral replication molecules, the I κ B α kinase kinase, IKKK, is activated over adaptor proteins like TRADD and TRAF2. It phosphorylates the multi enzyme complex I κ B α kinase (also called IKK) into its active form (the active form is referred herein as IKKa). Phosphorylation of I κ B α at its serine residues 32 and 36 by IKKa leads to its ubiquitination at lysine-21 and lysine-22 and fast degradation by the 26S-proteasome. Thereby set free NF- κ B exposes its nuclear localization sequence, which allows to translocate to the nucleus, to bind to κ B motifs present in the promoters of numerous genes, with it regulating their transcription. NF- κ B especially recognizes DNA elements with a consensus-sequence of 5'-GGGRNYYYCC-3' (and N is any nucleotide, R is any purine, Y is any pyrimidine), which consists of 5-base pair (bp) 5' subsite for p50 and 4 bp subsite for p65 [12]. NF- κ B activity is terminated by the newly synthesized I κ B α , which enters the nucleus, binds to NF- κ B and leads it out into cytoplasm.

IKK activity is thought to be transient, with fast increase at stimulation and rapidly decreasing thereafter. IKK inactivation is mainly controlled by the zincfinger protein A20, which is also vigorously NF- κ B responsive. This can be derived from the fact, that A20-deficient fibroblasts show persistent IKK activation after TNF stimulation. But the whole exact mechanisms of A20's action are not fully resolved at the moment . It could act in two ways: A20 could bind directly to IKKa effecting the kinase to turn into an inactive form IKKi. Or it may block the upstream transduction pathway between extracellular signal and IKK by binding to TNF receptor or associated adaptor proteins to block activation by those proteins. The used model contains the first kind of inhibition, although it

should have the same effect to use the other feedback possibility.

The model includes these two regulatory feedback loops involving $I\kappa B\alpha$ and A20. While $I\kappa B\alpha$ acts directly as an induced NF- κ B inhibitor, A20 terminates IKK activity leading to decreased $I\kappa B\alpha$ -degradation and is therefore an indirect inhibitor of NF- κ B. The applied model is created by Lipniacki et al. (2004) and includes two-compartment kinetics with a difference between the nuclear and the cytoplasmic volume.

The fitting process Lipniacki carried out "by hand", is arranged by comparison of values from model graphs with measured data from Lee et al. [9]. Estimation of 29 parameters for the model equations and 11 normalization factors needed for experimental data is accomplished using the optimization tool MUSCOD-II. Minimizing least squares terms, which consist of the difference between measured to modeled value in each measured point of time, by changing model parameters leads to the highest analogy of the two graphs.

With implementation of a hypothetical NF κ B induced target control gene into the model named cgen, quantitative specifications for mRNA transcription over time can be estimated after activation with an inducing component.

Figure 1 shows a schematic overview of the regulatory processes.

Table 1: Name and description of the model variables

Name	Description
IKKn	cytoplasmic concentration of neutral form of IKK kinase
IKKa	cytoplasmic concentration of active form of IKK
IKKi	cytoplasmic concentration of inactive form of IKK
$I\kappa B\alpha$	cytoplasmic concentration of $I\kappa B\alpha$
$I\kappa B\alpha_n$	nuclear concentration of $I\kappa B\alpha$
$I\kappa B\alpha_t$	concentration of $I\kappa B\alpha$ mRNA transcript
IKKa: $I\kappa B\alpha$	cytoplasmic concentration of complexes of IKKa and $I\kappa B\alpha$
$NF\kappa B_n:I\kappa B\alpha_n$	nuclear concentration of complexes of NF- κ B and $I\kappa B\alpha$;
$cgen_t$	mRNA of control gene
T_R	logical variable: if $T_R == 1$ extracellular activation signal is on, if $T_R == 0$ no signal is present
kv	= V/U - the ratio of cytoplasmic and nuclear volumes

2 Methods

In this model, 15 ordinary differential equations (ODEs) are used to model the regulatory network of NF- κ B. For more detailed information on the terms please see Lipniacki et al. (2004). Concentrations of mRNA transcripts of A20, $I\kappa B\alpha$ and $cgen$ are indexed with the subscript t, nuclear concentrations are denoted using the subscript n and complexes like $I\kappa B\alpha:NF\kappa B$ are combined with the sign "—" instead of ":" in mathematical formulas to avoid confusion. The model equations, annotations to the variables and parameters are shown in the following tables:

2.1 Model, Variables and Parameters

All variables used in the 15 ordinary differential equations modeling the NF κ B module are shown in the following table.

Throughout this article different notations for complexes are analogous: NF κ B is written instead of NF-kB or NF- κ B and (NF κ B— $I\kappa B\alpha$) instead of NF κ B: $I\kappa B\alpha$ in equations to avoid confusion.

In the following, the applied mathematical model of the two compartment, two negative feedback loop regulatory module is described by its 15 ordinary differential equations (see Ref. [1]).

$$\begin{aligned}
\frac{NF\kappa B}{dt} &= c_{6a}(I\kappa B\alpha|NF\kappa B) - a_1NF\kappa BI\kappa B\alpha \\
&\quad + t_2(IKKa|I\kappa B\alpha|NF\kappa B) - i_1NF\kappa B \\
\frac{NF\kappa B_n}{dt} &= i_1k_vNF\kappa B - a_1I\kappa B\alpha_nNF\kappa B_n \\
\frac{A20}{dt} &= c_4A20_t - c_5A20 \\
\frac{A20_t}{dt} &= c_2 + c_1NF\kappa B_n - c_3A20_t \\
\frac{IKKn}{dt} &= k_{prod} - k_{deg}IKKn - T_Rk_1IKKn \\
\frac{IKKa}{dt} &= T_Rk_1IKKn - k_3IKKa - T_Rk_2IKKaA20 \\
&\quad - k_{deg}IKKa - a_2IKKaI\kappa B\alpha + t_1(IKKa|I\kappa B\alpha) \\
&\quad - a_3IKKa(I\kappa B\alpha|NF\kappa B) + t_2(IKKa|I\kappa B\alpha|NF\kappa B) \\
\frac{IKKi}{dt} &= k_3IKKa + T_Rk_2IKKaA20 - k_{deg}IKKi \\
\frac{I\kappa B\alpha}{dt} &= -a_2IKKaI\kappa B\alpha - a_1I\kappa B\alpha NF\kappa B \\
&\quad + c_{4a}I\kappa B\alpha_t - c_{5a}I\kappa B\alpha - i_{1a}I\kappa B\alpha + e_{1a}I\kappa B\alpha_n \\
\frac{I\kappa B\alpha_n}{dt} &= -a_1I\kappa B\alpha_nNF\kappa B_n + i_{1a}k_vI\kappa B\alpha - e_{1a}k_vI\kappa B\alpha_n \\
\frac{I\kappa B\alpha_t}{dt} &= c_{2a} + c_{1a}NF\kappa B_n - c_{3a}I\kappa B\alpha_t \\
\frac{(IKKa|I\kappa B\alpha)}{dt} &= a_2IKKaI\kappa B\alpha - t_1(IKKa|I\kappa B\alpha) \\
\frac{(IKKa|I\kappa B\alpha|NF\kappa B)}{dt} &= a_3IKKa(I\kappa B\alpha|NF\kappa B) - t_2(IKKa|I\kappa B\alpha|NF\kappa B) \\
\frac{(I\kappa B\alpha|NF\kappa B)}{dt} &= a_1I\kappa B\alpha NF\kappa B - c_{6a}(I\kappa B\alpha|NF\kappa B) \\
&\quad - a_3IKKa(I\kappa B\alpha|NF\kappa B) + e_{2a}(I\kappa B\alpha_n|NF\kappa B_n) \\
\frac{(I\kappa B\alpha_n|NF\kappa B_n)}{dt} &= a_1I\kappa B\alpha_nNF\kappa B_n - e_{2a}k_v(I\kappa B\alpha_n|NF\kappa B_n) \\
\frac{cgen_t}{dt} &= c_{2c} + c_{1c}NF\kappa B_n - c_{3c}cgen_t
\end{aligned}$$

The model equations include the following parameters, which all are estimated within the optimization process and can be seen in an overview in Table 2.

Optimization was carried out with the optimization tool MUSCOD-II. To avoid numerical difficulties, every parameter was rescaled to a value between 1 and 100 only for optimization process in MUSCOD-II. The rescaled values were multiplied with the scaling factors before taken into the equations. The derivatives had of course finally to be divided by the according scale factor, so that throughout the equation system the original values could be used.

There were 11 measurements over time from Lee's experiments (Lee et al. 2000) consisting of A20 mRNA for wildtype cells and total amount of IKK, active IKKa, cytoplasmic I κ B α , nuclear NF- κ B and I κ B α mRNA for both wildtype and A20 deficient cells during persistent TNF stimulation.

To compare measurements and model response for the total amount of IKK, which is not a variable itself in the equations, the sum of IKKa, IKKi and IKKn was used within the least squares terms. In the same manner, data for total amount of I κ B α were compared with the sum of variables containing I κ B α , i.e. IKKa:I κ B α , IKKa:I κ B α :NF κ B, cytoplasmic I κ B α and cytoplasmic IKKa:I κ B α :NF κ .

Measurements were not all conducted in the same points in time, so the residual values at missing points were set to zero. This is automatically done by the implementation when the measurement value was set to -1.

Results of given experimental data were just semi-quantitative because of lack of comparable standard measurements with known amounts. The achieved absolute values had to be normalized and thus the available data consists of values from 0 to 1. The needed 11 normalization factors were also taken into account for optimization and are referred herein as $m_1 - m_{11}$. To obtain a physiologically meaningful initial set, the highest graph values of the predetermined model for each given variable were put in to start the optimization. The concordant points in time of the highest values all were found corresponding to the time belonging to value 1 in experimental data, indicating a reasonable procedure. Afterwards they were set free to be optimized in further processing.

To achieve a steady state at the beginning, the simulation was conducted without external signal (logical variable set to $T_R = 0$) for a long time of 6060

Table 2: **Name and description all model parameters**

Parameter	Description
kv	=V/U ratio of cytoplasmic and nuclear volumes
k_{prod}	de novo synthesis rate for IKK η
k_{deg}	degradation rate for all IKK
a_1	rate of NF κ B + I κ B α to NF κ B:I κ B α
a_2	rate of IKKa + I κ B α to IKKa:I κ B α
a_3	rate of IKKa + I κ B α :NF κ B to IKKa:I κ B α :NF κ B
c_1	NF κ B - induced transcription rate of A20 $_t$ (=A20-mRNA)
c_2	constitutive transcription rate of A20 $_t$ (=A20-mRNA)
c_3	degradation rate of A20 $_t$
c_4	synthesis rate A20 $_t$ (=A20-mRNA) to A20
c_5	constitutive degradation rate of A20
c_{1a}	NF κ B-induced transcription rate of I κ B α_t (=I κ B α -mRNA)
c_{2a}	constitutive transcription of rate I κ B α_t (=I κ B α -mRNA)
c_{3a}	degradation rate of I κ B α
c_{4a}	synthesis rate I κ B α_t to I κ B α
c_{5a}	constitutive degradation rate of I κ B α
c_{6a}	rate NF κ B:I κ B α to NF κ B + I κ B α (degraded)
c_{1c}	NF κ B-induced transcription rate of cgen $_t$ (=control gene mRNA)
c_{2c}	constitutive transcription rate of cgen $_t$ (=control gene mRNA)
c_{3c}	degradation rate of cgen $_t$
e_{1a}	transport-rate "ex"/out of the nucleus for I κ B α
e_{2a}	transport-rate "ex"/out of the nucleus for I κ B α :NF κ B
i_1	transport-rate into nucleus for NF κ B
i_{1a}	transport-rate into nucleus for I κ B α
k_1	rate IKK η to IKKa
k_2	rate IKKa to IKKi with A20
k_3	rate IKKa to IKKi sponanteous
t_1	rate IKKa:I κ B α to IKKa + I κ B α
t_2	rate IKKa:I κ B α :NF κ B to IKKa + I κ B α :NF κ B

Table 3: Name and steady state values for the model variables using Lipniacki's suggestions

Name of Variable	Steady state value	Units
NF- κ B	3.156	$\times 10^{-4} \mu\text{M}$
NF- κ B _n	2.297	$\times 10^{-3} \mu\text{M}$
A20	4.777	$\times 10^{-3} \mu\text{M}$
A20 _t	2.865	$\times 10^{-3} \mu\text{M}$
IKK η	1.998	$\times 10^{-1} \mu\text{M}$
IKK α	0	μM
IKK β	0	μM
I κ B α	2.504	$\times 10^{-3} \mu\text{M}$
I κ B α _n	3.433	$\times 10^{-3} \mu\text{M}$
I κ B α _t	2.865	$\times 10^{-3} \mu\text{M}$
IKK α :I κ B α	0	μM
IKK α :NF κ B:I κ B α	0	μM
I κ B α :NF κ B	5.921	$\times 10^{-2} \mu\text{M}$
I κ B α :NF κ B _n	7.884	$\times 10^{-5} \mu\text{M}$
cgen _t	2.865	$\times 10^{-6} \mu\text{M}$

minutes according to 101 hours in Lipniacki's procedure. The system went into a steady state and these values of the variables could be set as initial conditions for the following procedure. Trials with other starting values always resulted in same steady state values. Only the total amount of NF- κ B had to be adjusted to $0.06 \mu\text{M}$ according to estimated guidelines from Lipniacki due to the fact that other amounts of this variable would lead to other steady states. It did not make a difference in which form NF- κ B was initially present. The steady state values can be seen in Table 3.

With these values the simulation of the start of cellular response was carried out by switching the variable T_R from 0 to 1. For the following simulation 9 model stages were used, each with its start point exactly at the measurement time points at 0, 10, 20, 30, 60, 90, 120, 150 and 180 minutes. Thus, model and measured data could be easily compared in each model stages starting point.

To optimize parameters for given experimental data of both wildtype and A20 deficient cells in the same procedure, the simulation was repeated after 180 minutes again starting with a longer period without external signal to achieve steady

state. To compare the model with data from A20 deficient cells, the variables A20 and $A20_t$ were set to 0 by introducing a differential equation $\frac{dx}{dt} = -x$. This leads to a fast decrease to 0 during the second steady state adjusting period. Thus, simulating conditions as in A20 deficient "knock out" cells, the model could be used for a second simulation, this time compared with A20 deficient cell data. Changing parameters had an influence on both systems, so the optimization software could take into account all of the given data at the same time.

The objective function was defined by least squares terms which consist of the difference between values of model trajectories and experimental data at all available points of time. These values are squared to gain only positive values and then added up in one sum. If no experimental data was available for a variable at any point of time, the missing difference was set to zero.

During the procedure, 40 parameters and normalization factors had to be revised. Only 11 measurements for 15 variables i.e. altogether 165 measurements could be utilized. To regularize the problem during the first iteration steps, a second term was added to the objective function to help the optimizing software not to adopt unphysiological values. It contained the sum of differences between all current values of the 40 used parameters and the proposed values from Lipniacki's results (see Ref. [1]). This sum was weighted to allow a later on reduction of the influence of this second part onto the objective function in further iteration steps. The weight could easily be changed at each step of the process.

To hold some parameters in already experimentally approved meaningful values, upper and lower bounds for the optimization tool could be set. Thus, for a_1 (association rate of $NF\kappa B + I\kappa B\alpha$ to $NF\kappa B:I\kappa B\alpha$) an interval from 4 to $6 \times 10^{+5}$ M/s was chosen according to Hoffmann's suggestion of $5 \times 10^{+5}$ M/s. The parameter k_v describing the relation of cytoplasmic to nuclear volume was limited to values between 1 and 6. Also c_2 (constitutive transcription rate of A20-mRNA) and c_{2a} (constitutive transcription rate of $I\kappa B\alpha$ -mRNA) should only increase to values up to 1.5×10^{-9} M/s analogous to calculations of Lipniacki, so this value was placed as maximum bound. c_{3a} was given an interval of 30 - 50 1/s and c_{5a} (constitutive degradation rate of $I\kappa B\alpha$) and c_{6a} (rate $NF\kappa B:I\kappa B\alpha$ to $NF\kappa B + I\kappa B\alpha$ (degraded)) were bound to 1×10^{-5} 1/s until 1×10^{-3} 1/s appropriate to suggested values of 1×10^{-4} 1/s and 2×10^{-5} 1/s by Pando and Verma (references all in Lipniacki et al. 2004).

2.2 (A) Lipniacki's parameters with optimized normalization factors

The first step in adapting the system to measured data was the estimation of 11 normalization factors. It was carried out with fixed set of parameters using Lipniacki's suggestions. Each normalization factor was estimated and changed until the objective function value was minimized. Thereby it did not matter whether all 11 factors were set free at the same time since they do not influence each other. The first set of values for the normalization factors can be seen in the first column in Table 4.

2.3 (B) Optimization of parameters with fixed normalization factors

Providing a fundament to start the optimization with, the obtained normalization factors were fixed and the parameters were set free one after another. To be able to change many parameters at the same time, the weight for the second term was fixed to 1×10^{-1} . After convergence more parameters were set free until all 29 could be changed at the same time. If problems with small values or too many degrees of freedom occurred, the one relevant parameter was optimized with most of the others fixed for a few iterations.

2.4 (C) Optimization of both parameters and normalization factors

By the time that all parameters were free at the same time, also the normalization factors were set free for changing and the weight for the second part of the objective function was slowly lowered in a way, that degrees of freedom were yet restrained and convergence could be achieved. Repeating this step several times, the weight could be decreased to a value of 0 and therefore fully free selectable sets of parameters.

Thus, the objective function to be minimized contained two kinds of least squares terms, one for comparison of the model with measured data and the other to start parameter estimation with Lipniacki's suggestions allowing more freedom during the progress of optimization.

3 Results

3.1 Parameter estimation

Having set all 40 parameters free for optimization, most of them were changed by MUSCOD-II and the objective function was minimized. Comparing Lipniacki's assumptions with the new suggestions shown in the two tables below, it can be seen that some estimations were confirmed, while other values differ clearly from the proposal. Especially c_{1a} (NF κ B-induced transcription rate of I κ B α -mRNA), c_{2a} (constitutive transcription rate of I κ B α -mRNA) and c_{3a} (degradation rate of I κ B α) respectively, showed analogy to Lipniacki's assumption. Furthermore k_3 (rate of spontaneous transition of IKKa to IKKi) was validated with values similar to the proposal (for comparison see Table 4 and 5 below).

Exact values (i.e. 10.00 1/s) of some optimized parameters indicate a reached bound during estimation process. It shows that setting physiological meaningful bounds has an impact on the results. This effect can be observed in values for $k_v = 1.00$ (ratio of cytoplasmic and nuclear volumes), $c_2 = 1.5 \times 10^{-9}$ M/s (constitutive transcription rate of A20-mRNA), $c_{3a} = 50$ 1/s (degradation rate of I κ B α) and $c_{6a} = 30$ 1/s (as rate of NF κ B:I κ B α to NF κ B + I κ B α) (see also Table 5).

Some other parameters were changed to implausible values, like a_3 (rate of IKKa + I κ B α :NF κ B to IKKa:I κ B α :NF κ B) with increase from 10 to 1000 $\times 10^{-1}$ 1/ μ Ms, e_{1a} (transport rate out of nucleus for I κ B α) with increase of 50 to 1331 $\times 10^{-5}$ 1/s or k_1 (transition rate of IKKn to IKKa) increasing from 25 to 496.9 $\times 10^{-4}$ 1/s. Further investigations will indicate whether those parameters should be given a bound during the optimization.

3.2 (A) Lipniacki's parameters with optimized normalization factors

Adapting the system to measured data by the estimation of the 11 normalization factors led to the first complete set of all 40 values to be estimated. The values for the normalization factors can be seen in the first column in Table 4 together with parameter values from Lipniacki [1]. The value of objective function after this first step of estimation was 3.35, which can be taken as a reference for the following optimization processes.

3.3 (B) Optimization of parameters with fixed normalization factors

Now, all 29 parameters were set free successively, keeping the normalization factors fixed to their obtained values. Since therefore all parameters were optimized, the objective function fell to a value of 1.96. Values were yet constrained by the second term in objective function keeping them near the original proposal. The appropriate set of parameters and normalization factors can be seen in the second column in 4.

3.4 (C) Optimization of both parameters and normalization factors

By the time all parameters and normalization factors were free at the same time, the weight for the second part of the objective function was slowly lowered in a way, that degrees of freedom were yet restrained and convergence could be achieved. Repeating this step several times, the weight could be decreased to a value of 0 and therefore a fully free selectable sets of parameters. This led once again to a decreased value of the objective function of 1.32. The final set of optimized parameters and normalization factors is shown in the second column in Fig. 5.

Solving system equations with the newly assumed parameter set produced a temporal evolution of variables for wildtype and A20 deficient cells.

They can be compared to experimental data graphs, which show the semi-quantitative values already multiplied by the estimated normalization factors to be able to compare also quantitative behavior. They are shown at the end of this document.

Changing the ratio of nuclear and cytoplasmic volumes by altering the parameter k_v (which represents this ratio) shows different response profiles. This could give an explanation to changing cell responses during maturation of cells, in which the ratio of cytoplasmic to nuclear volume increases. It could be used to analyse models for different stages in development and taken into account for design of drugs that target onto fast developing cells as in tumors to eventually predict different effects of the same amount of therapeutic agents on cells in different

Table 4: **Results of first step new suggestions of calculated parameter and normalization factors (B) in comparison with Lipniacki's assumptions (A)**

Name	Description of parameter	(A)	(B)	Units
kv	=V/U ratio of cytoplasmic and nuclear volumes	5	4.47	–
k_{prod}	de novo synthesis rate for IKKn	25	85.13	$10^{-6}\mu\text{M/s}$
k_{deg}	degradation rate for all IKK	12.5	43.20	$10^{-5}1/\text{s}$
a_1	rate of $\text{NF}\kappa\text{B} + \text{I}\kappa\text{B}\alpha$ to $\text{NF}\kappa\text{B}:\text{I}\kappa\text{B}\alpha$	50	40.00	$10^{-2}1/\mu\text{Ms}$
a_2	rate of $\text{IKKa}+\text{I}\kappa\text{B}\alpha$ to $\text{IKKa}:\text{I}\kappa\text{B}\alpha$	20	20.96	$10^{-2}1/\mu\text{Ms}$
a_3	rate of $\text{IKKa}+\text{I}\kappa\text{B}\alpha:\text{NF}\kappa\text{B}$ to $\text{IKKa}:\text{I}\kappa\text{B}\alpha:\text{NF}\kappa\text{B}$	10	1.32	$10^{-1}1/\mu\text{Ms}$
c_1	$\text{NF}\kappa\text{B}$ -induced transcription rate of A20_t	50	86.71	$10^{-8}1/\text{s}$
c_2	constitutive transcription rate of A20-mRNA	0	0	10^{-9}M/s
c_3	degradation rate of A20-mRNA	40	118.10	$10^{-5}1/\text{s}$
c_4	synthesis rate A20-mRNA to A20	50	328.15	$10^{-2}1/\text{s}$
c_5	constitutive degradation rate of A20	30	80.40	$10^{-5}1/\text{s}$
c_{1a}	$\text{NF}\kappa\text{B}$ -induced transcription rate of $\text{I}\kappa\text{B}\alpha_t$	50	48.97	$10^{-8}1/\text{s}$
c_{2a}	constitutive transcription of rate $\text{I}\kappa\text{B}\alpha_t$	0	0	10^{-9}M/s
c_{3a}	degradation rate of $\text{I}\kappa\text{B}\alpha$	40	50.00	$10^{-5}1/\text{s}$
c_{4a}	synthesis rate $\text{I}\kappa\text{B}\alpha_t$ to $\text{I}\kappa\text{B}\alpha$	50	47.07	$10^{-2}1/\text{s}$
c_{5a}	constitutive degradation rate of $\text{I}\kappa\text{B}\alpha$	10	20.00	$10^{-5}1/\text{s}$
c_{6a}	rate $\text{NF}\kappa\text{B}:\text{I}\kappa\text{B}\alpha$ to $\text{NF}\kappa\text{B} + \text{I}\kappa\text{B}\alpha$ (degraded)	20	30.00	$10^{-6}1/\text{s}$
c_{1c}	$\text{NF}\kappa\text{B}$ -induced transcription rate of cgen_t	50	86.71	$10^{-8}1/\text{s}$
c_{2c}	constitutive transcription rate of cgen_t	0	0	10^{-9}M/s
c_{3c}	degradation rate of cgen_t	40	118.10	$10^{-5}1/\text{s}$
e_{1a}	transport rate out of nucleus for $\text{I}\kappa\text{B}\alpha$	50	756.57	$10^{-5}1/\text{s}$
e_{2a}	transport rate out of nucleus for $\text{I}\kappa\text{B}\alpha:\text{NF}\kappa\text{B}$	10	9.00	$10^{-3}1/\text{s}$
i_1	transport rate into nucleus for $\text{NF}\kappa\text{B}$	25	167.25	$10^{-4}1/\text{s}$
i_{1a}	transport rate into nucleus for $\text{I}\kappa\text{B}\alpha$	10	3.56	$10^{-4}1/\text{s}$
k_1	rate IKKn to IKKa	25	234.09	$10^{-4}1/\text{s}$
k_2	rate IKKa to IKKi with A20	10	2.96	$10^{-2}1/\text{s}$
k_3	rate IKKa to IKKi sponanteous	15	19.52	$10^{-4}1/\text{s}$
t_1	rate $\text{IKKa}:\text{I}\kappa\text{B}\alpha$ to $\text{IKKa} + \text{I}\kappa\text{B}\alpha$	10	131.60	$10^{-2}1/\text{s}$
t_2	rate $\text{IKKa}:\text{I}\kappa\text{B}\alpha:\text{NF}\kappa\text{B}$ to $\text{IKKa} + \text{I}\kappa\text{B}\alpha:\text{NF}\kappa\text{B}$	10	0.32	$10^{-2}1/\text{s}$
	objective function value	3.35	1.96	–
m_1	Norm. factor for A20 mRNA wildtype meas.	1.81	1.81	$10^{-4}\mu\text{M}$
m_2	Norm. factor for total IKK wildtype meas.	0.251	0.251	μM
m_3	Norm. factor for IKKa wildtype meas.	0.0736	0.0736	μM
m_4	Norm. factor for $\text{I}\kappa\text{B}\alpha$ wildtype meas.	0.108	0.108	μM
m_5	Norm. factor for nucl. $\text{NF}-\kappa\text{B}$ wildtype meas.	0.257	0.257	μM
m_6	Norm. factor for $\text{I}\kappa\text{B}\alpha$ mRNA wildtype meas.	1.67	1.67	$10^{-4}\mu\text{M}$
m_7	Norm. factor for total IKK A20deficient meas.	0.266	0.266	μM
m_8	Norm. factor for IKKa A20deficient meas.	0.0827	0.0827	μM
m_9	Norm. factor for $\text{I}\kappa\text{B}\alpha$ A20deficient meas.	0.0782	0.0782	μM
m_{10}	Norm. factor for nucl. $\text{NF}-\kappa\text{B}$ A20def. meas.	0.266	0.266	μM
m_{11}	Norm. factor for $\text{I}\kappa\text{B}\alpha$ mRNA A20def. meas.	2.95	2.95	$10^{-4}\mu\text{M}$

Table 5: **Results of second step suggestions of calculated parameter and normalization factors (C) in comparison with first step assumptions (B)**

Name	Description of parameter	(B)	(C)	Units
kv	=V/U ratio of cytoplasmic and nuclear volumes	4.47	1.00	–
k_{prod}	de novo synthesis rate for IKKn	85.13	64.20	$10^{-6}\mu\text{M/s}$
k_{deg}	degradation rate for all IKK	43.20	36.83	$10^{-5}1/\text{s}$
a_1	rate of $\text{NF}\kappa\text{B} + \text{I}\kappa\text{B}\alpha$ to $\text{NF}\kappa\text{B}:\text{I}\kappa\text{B}\alpha$	40.00	60.00	$10^{-2}1/\mu\text{Ms}$
a_2	rate of $\text{IKKa}+\text{I}\kappa\text{B}\alpha$ to $\text{IKKa}:\text{I}\kappa\text{B}\alpha$	20.96	15.48	$10^{-2}1/\mu\text{Ms}$
a_3	rate of $\text{IKKa}+\text{I}\kappa\text{B}\alpha:\text{NF}\kappa\text{B}$ to $\text{IKKa}:\text{I}\kappa\text{B}\alpha:\text{NF}\kappa\text{B}$	1.32	100.00	$10^{-1}1/\mu\text{Ms}$
c_1	$\text{NF}\kappa\text{B}$ -induced transcription rate of A20_t	86.71	419.68	$10^{-8}1/\text{s}$
c_2	constitutive transcription rate of A20-mRNA	0	1.50	$10^{-9}\mu\text{M/s}$
c_3	degradation rate of A20-mRNA	118.10	161.11	$10^{-5}1/\text{s}$
c_4	synthesis rate A20-mRNA to A20	328.15	501.74	$10^{-2}1/\text{s}$
c_5	constitutive degradation rate of A20	80.40	566.09	$10^{-5}1/\text{s}$
c_{1a}	$\text{NF}\kappa\text{B}$ -induced transcription rate of $\text{I}\kappa\text{B}\alpha_t$	48.97	46.39	$10^{-8}1/\text{s}$
c_{2a}	constitutive transcription of rate $\text{I}\kappa\text{B}\alpha_t$	0	0	$10^{-9}\mu\text{M/s}$
c_{3a}	degradation rate of $\text{I}\kappa\text{B}\alpha$	50.00	50.00	$10^{-5}1/\text{s}$
c_{4a}	synthesis rate $\text{I}\kappa\text{B}\alpha_t$ to $\text{I}\kappa\text{B}\alpha$	47.07	222.05	$10^{-2}1/\text{s}$
c_{5a}	constitutive degradation rate of $\text{I}\kappa\text{B}\alpha$	20.00	17.36	$10^{-5}1/\text{s}$
c_{6a}	rate $\text{NF}\kappa\text{B}:\text{I}\kappa\text{B}\alpha$ to $\text{NF}\kappa\text{B} + \text{I}\kappa\text{B}\alpha$ (degraded)	30.00	30.00	$10^{-6}1/\text{s}$
c_{1c}	$\text{NF}\kappa\text{B}$ -induced transcription rate of cgen_t	86.71	419.68	$10^{-8}1/\text{s}$
c_{2c}	constitutive transcription rate of cgen_t	0	1.50	$10^{-9}\mu\text{M/s}$
c_{3c}	degradation rate of cgen_t	118.10	161.11	$10^{-5}1/\text{s}$
e_{1a}	transport rate out of nucleus for $\text{I}\kappa\text{B}\alpha$	756.57	1331.23	$10^{-5}1/\text{s}$
e_{2a}	transport rate out of nucleus for $\text{I}\kappa\text{B}\alpha:\text{NF}\kappa\text{B}$	9.00	2.01	$10^{-3}1/\text{s}$
i_1	transport rate into nucleus for $\text{NF}\kappa\text{B}$	167.25	58.56	$10^{-4}1/\text{s}$
i_{1a}	transport rate into nucleus for $\text{I}\kappa\text{B}\alpha$	3.56	1.00	$10^{-4}1/\text{s}$
k_1	rate IKKn to IKKa	234.09	496.99	$10^{-4}1/\text{s}$
k_2	rate IKKa to IKKi with A20	2.96	378.13	$10^{-2}1/\text{s}$
k_3	rate IKKa to IKKi sponanteous	19.52	14.37	$10^{-4}1/\text{s}$
t_1	rate $\text{IKKa}:\text{I}\kappa\text{B}\alpha$ to $\text{IKKa} + \text{I}\kappa\text{B}\alpha$	131.60	128.96	$10^{-2}1/\text{s}$
t_2	rate $\text{IKKa}:\text{I}\kappa\text{B}\alpha:\text{NF}\kappa\text{B}$ to $\text{IKKa} + \text{I}\kappa\text{B}\alpha:\text{NF}\kappa\text{B}$	0.32	0.37	$10^{-2}1/\text{s}$
	objective function value	1.96	1.32	–
m_1	Norm. factor for A20 mRNA wildtype meas.	1.81	1.62	$10^{-4}\mu\text{M}$
m_2	Norm. factor for total IKK wildtype meas.	0.251	0.229	μM
m_3	Norm. factor for IKKa wildtype meas.	0.0736	0.00093	μM
m_4	Norm. factor for $\text{I}\kappa\text{B}\alpha$ wildtype meas.	0.108	0.201	μM
m_5	Norm. factor for nucl. $\text{NF}-\kappa\text{B}$ wildtype meas.	0.257	0.0604	μM
m_6	Norm. factor for $\text{I}\kappa\text{B}\alpha$ mRNA wildtype meas.	1.67	0.451	$10^{-4}\mu\text{M}$
m_7	Norm. factor for total IKK A20deficient meas.	0.266	0.235	μM
m_8	Norm. factor for IKKa A20deficient meas.	0.0827	0.0911	μM
m_9	Norm. factor for $\text{I}\kappa\text{B}\alpha$ A20deficient meas.	0.0782	0.110	μM
m_{10}	Norm. factor for nucl. $\text{NF}-\kappa\text{B}$ A20def. meas.	0.266	0.0613	μM
m_{11}	Norm. factor for $\text{I}\kappa\text{B}\alpha$ mRNA A20def. meas.	2.95	0.585	$10^{-4}\mu\text{M}$

developing stages.

3.5 Comparison of model and measured data graphs

Comparing the graphs of model prediction for wild type cells (see Fig.3) with trajectories for measured values (see Fig.5 and 6), most of the trajectories describe the time evolution characteristics and the quantity of the values well.

A20 mRNA predictions of the model comply with experimental data in temporal behavior as well as in concentrations (compare Fig.5 panel [A] with Fig.3 panel I). Since measurements took place during first two hours, only these times can be compared.

The total amount of IKK, which shows a slight oscillation around concentrations of $0.2 \mu\text{M}$ in the measurements (see Fig.5 panel [B]) matches with the sum of IKKa, IKKi and IKKn (see Fig.3 panels A, B and C), which is also near $0.2 \mu\text{M}$.

Trajectories for $I\kappa B\alpha$ (compare Fig.5 panel [F] with Fig.3 panel J) is in accordance of temporal devolution, only the peak value at 90 minutes differs from 0.2 to $0.15 \mu\text{M}$. The course of $I\kappa B\alpha$ -mRNA in model and measurement is in absolute compliance as it can be seen in Fig.6 panel [J] and Fig.3 panel L).

The lapse of nuclear NF- κ B shows analogue quantitative behavior, missing a small valley at 20 minutes and a flat peak at 120 minutes (Fig.6 panel [H] with Fig.3 panel G). Nevertheless, the underlying main oscillation is in conformance with experimental data.

Predictions for IKKa in wildtype cells match in time and quantitative behavior of the later steady state values. The only difference between model and experiment seems to be the sharpness of the beginning peak. It is lowered in given data and much more excessive in model predictions. This may be derived from non-linear measurement methods, which "cut off" higher concentration values. Two strategies to solve this problem can be offered. On the one hand, more linear marking dyes can be applied for producing experimental data with longer linear intensity in higher concentrations, which would change the data graph to be compared to. On the other hand, non-linear dulling of peak-intensity in high concentrations can be implemented into the model in future updates.

The same effect occurs for progression of IKKa in A20 deficient cells, as it can be seen in Fig.5 panel [E] in comparison to Fig.4 panel B. Again, the height of the first peak is lower than in the model, but quantitative trend and a steady

state value of $0.04\mu\text{M}$ at 100 minutes fit very well.

Also predictions for amount of total IKK in A20 deficient cells is in absolute congruence to measured data, starting at 0 minutes with $0.17\mu\text{M}$ IKKn (Fig.5 panel [C] and Fig.4 panel A), over $0.23\mu\text{M}$ at 30 minutes (total IKK in Fig.5 panel [C] versus IKKa + IKKi in Fig.4 panel B and C) to an equilibrium state after 120 minutes of $0.14\mu\text{M}$ (Fig.5 panel [C] and Fig.4 panel C).

The lapse of $I\kappa\text{B}\alpha$ (compare Fig.5 panel [G] with Fig.4 panel J) shows the same end value around $0.02\mu\text{M}$ from 1 hour on, but experimental data does not contain a minimum in concentration at 20 minutes as distinct as the model predicts.

Whereas predictions for $I\kappa\text{B}\alpha$ mRNA (Fig.6 panel [K] and Fig.4 panel L) and nuclear NF- κB (Fig.6 panel [I] and Fig.4 panel G) for A20 deficient cells show exactly the same temporal behavior in both model and measured data graphs.

4 Conclusions and Outlook

With the procedure as described above, all 40 parameters can be set free for optimization at the same time. Given only 11 measurements at different timesteps, there are a lot of degrees of freedom for the program to produce a solution. The system can be adapted very easily to measurements for more points in time, which can be implemented by increasing the number of stages. In addition, more measurements of other variables can be taken into account, especially data for main regulatory proteins like A20 or IKKn important for steady state value estimation. Supported by the chance of more comparable measured data, the procedure could estimated parameters much better and therefore give more precise predictions. Additionally, other series of measurements of, for instance, 15 or 30 minutes of stimulation with TNF could be added like A20 deficient series to be able to compare model and data in more than just persistent stimulation conditions. Implementation of more data can be attained fast and easily and will be one of the first goals for future work.

Estimations for most parameters were conducted without any bounds. But some values increased to unphysiological amounts, so that optimization in more limited ranges leading to more meaningful results would contribute to supposedly correct assumptions emerged from experiments in the last years. Hoffmann et al. give some proposal to degradation and association rates (see Ref. [13]), so

physiological bounds could be derived from those suggestions resulting in higher validity. To retain values of these parameters close to assumptions in future applications could affect optimization of the others in a way to gain a set of parameters even closer to objectivity.

The optimal set of parameters was received while starting with Lipniacki's suggestion. Application of described method with different initial values could result in one or more different optimal sets for parameter. Whether the herein achieved set of parameter is the only solution or if there are several meaningful sets for the same conditions and bounds will be topic of further research.

Experimental data as well as the numerical method lack a specification of errors. For the optimization process an error could be derived and estimated from intensities of oscillations during the change of parameters in each iteration step. Low oscillating parameter values indicate a stable parameter, which would result in low error estimation. But since experimental errors appear even greater, they have to be determined in the first step.

The activation signal imitating $\text{TNF}\alpha$ binding and signal transduction switches from 0 to 1 when activation is started. A sigmoidal activation function would be more physiological. This can be integrated in further enhancements.

For the future, this signal pathway can be combined with models of preceding and parallel processes to achieve an even more accurate quantitative prediction model for regulatory activities and transcription or translation induced by $\text{NF-}\kappa\text{B}$ and $\text{TNF}\alpha$.

4.1 Applications

Computer-based, exact estimation of parameters for the $\text{NF-}\kappa\text{B}$ module can validate and optimize models that in future could produce not only qualitative, but also quantitative predictions for state of activation, gene expression, concentration and properties of physiological factors as well as therapeutical agents changing over time.

Nuclear factor κB plays an prominent integrating role as a transcription factor in the regulation of immune response, inflammation and cell cycle regulation. As an example, $\text{NF-}\kappa\text{B}$ is important in processes of lymphocyte activation, survival and normal immune responses. Regulating the transcription of inflammatory genes, the $\text{NF-}\kappa\text{B}$ activation pathway represents attractive targets for developing

anti-inflammatory therapeutics.

It is activated by various extracellular stimuli like inflammatory cytokines and other immune stimuli, viruses and oxidants. Bound to its recognition elements it induces proinflammatory cytokines, chemokines, Nitric Oxide (see Ref. [2]), antimicrobial peptides, stress response proteins and antiapoptotic proteins beneath inflammatory enzymes (see Ref. [3]) and adhesion molecules (such as intercellular adhesion molecule-1 (ICAM-1) expressed in the gut following traumatic brain injury (see Ref. [4])).

A fundamental inhibitor class are glucocorticoids, that inhibit activated NF- κ B, which seems to be important in the anti-inflammatory action of steroids. Novel inhibitors of NF- κ B are under development for treatment of inflammatory diseases (see Ref. [5]). Current pre-clinical studies point onto this capability of specific NF- κ B inhibitors in the clinical use (see Ref. [6]).

Constitutive activation of NF- κ B pathways is often associated with inflammatory diseases like rheumatoid arthritis, inflammatory bowel disease, multiple sclerosis, and asthma (see Ref. [3]). Additionally, the nuclear translocation of transcription factors may have influence on formation of ischaemia/ reperfusion (I/R) injury. NF- κ B participates in the cascade of events leading to TNF α production leading to neutrophil recruitment, tissue injury and lethality following intestinal I/R (see Ref. [7]).

Since one focus of current diabetes research is the clarification of the relationship between inflammation and diabetes, this approach is in the need of descriptive models for inflammation processes as well. Even minimal disturbances in glucose tolerance are associated with a chronic, generalized inflammatory reaction in which again the most important mediators and markers of this inflammation cascade are NF- κ B and TNF α (see Ref. [6]).

At least, the influence on the cell cycle has lead the focus of anti cancer development onto inhibitors of this module. As an example, most of nonsmall cell lung cancer (NSCLC) show dysregulated antiapoptotic pathways involving NF- κ B. In addition, in NSCLC both chemotherapy and radiation upregulate antiapoptotic and cell-cycle regulatory proteins through NF- κ B-dependent signaling mechanisms. Inhibition of NF- κ B dampes the resistance of NSCLC to undergo apoptosis and therefore sensitizes these cells to chemotherapy, as phase I clinical trials denote. Modulation of the antiapoptotic cascade mediated by NF- κ B, combined with either traditional or novel chemotherapeutic agents, seem to represent a promising future treatment strategy for patients with NSCLC (see Ref. [8]).

Validation and Optimization of the models for NF- κ B regulation in its dy-

dynamic module can provide a platform for both better understanding and more precise predictions of physiological processes, but also can give suggestions for target enzymes or mRNA. Hypotheses for preferably effective points of application for inhibitors could be established cost- and timesaving in silico and verified with experiments.

The temporal evolution of activated transcription of a NF- κ B induced gene after stimulation can be evaluated by comparing it with the integrated hypothetical control gene cgen.

Having decreased the objective function to about one third from 3.35 to 1.32 indicates success in the numerical optimization using MUSCOD-II. The method has been developed completely and is working, able to estimate many parameters to optimize the given model. With upgrades like more data to be taken into account or more parameters bound to physiologically reasonable values it will hopefully help to improve theoretical concepts and practical applications for fundamental research and drug development.

5 Acknowledgements

I would like to thank Dr. Anna Marciniak for always speedy support in getting experimental and model data, her help with LateX and for her idea to carry out this project.

For his enduring and skilled help with implementation and debugging of the model in MUSCOD-II and the development of the successful optimization method as well as accurately revising of this report I would like to give a lot of thanks to Dr. Moritz Diehl.

In addition, I thank Felix Bonowski for providing fast and very useful assistance with implementation of the model in C and Johannes Horlemann for finding this topic between the hardly connected fields of biology and optimization.

Last but not least I would like thank Stefan Quint very much for revising my report and for his continuous support and his kindhearted help in critical moments.

References

- [1] Lipniacki T, Paszek P, Brasier A, Luxon B, Kimmel M: *Mathematical model of NF- κ B regulatory model*. Journal of Theoretical Biology. 228 (2004) 195-215 and references therein.
- [2] Bai Y, Onuma H, Bai X, Medvedev AV, Misukonis M, Weinberg JB, Cao W, Robidoux J, Floering LM, Daniel KW, Collins S. *Persistent NF- κ B activation in Ucp2-/-mice leads to enhanced nitric oxide and inflammatory cytokine production*. J Biol Chem. (2005 Mar 9).
- [3] Verma I M. *Nuclear factor (NF)- κ B proteins: therapeutic targets*. Annals of the Rheumatic Diseases (2004):63 ii57-ii61.
- [4] Hang CH, Shi JX, Li JS, Li WQ, Yin HX. *Up-regulation of intestinal nuclear factor kappa B and intercellular adhesion molecule-1 following traumatic brain injury in rats*. World J Gastroenterol. (2005 Feb 28), 11(8):1149-54.
- [5] Barnes PJ. *Nuclear factor-kappa B*. Int J Biochem Cell Biol. (1997) Jun, 29(6):867-70.
- [6] Celec P. *Nuclear factor kappa B - molecular biomedicine: the next generation*. Biomed Pharmacother. (2004) Jul-Aug, 58(6-7):365-71.
- [7] Souza DG, Vieira AT, Pinho V, Sousa LP, Andrade AA, Bonjardim CA, McMillan M, Kahn M, Teixeira MM. *NF-kappaB plays a major role during the systemic and local acute inflammatory response following intestinal reperfusion injury*. Br J Pharmacol. (2005) Mar 14.
- [8] Semin. Thorac Cardiovasc Surg. (2004) Spring, 16(1):28-39.
- [9] Lee E G, Boone D, Chai S, Libby S L, Chien M, Lodolce J, Ma A. *Failure to regulate TNF-induced NF-kB and cell death responses in A20-deficient mice*. (2000) Science 289, 2350-2354.
- [10] Alberts et al. *molecular biology of the cell*, 4th edition, p898f.
- [11] Diehl M, Leineweber D, Schaefer A. *Muscod-II Users' Manual*, Preprint 2001-25, June (2001) .
- [12] Chen FE, Huang D, Chen Y, Ghosh G. *Crystal structure of p50/p65 heterodimer of transcription factor NF-kB bound to DNA*. (1998), Nature 391, 410-413.

- [13] Hoffmann H, Levchenko A, Martin LS, Baltimore D. *The I κ B-NF- κ B Signaling Module: Temporal Control and Selective Gene Activation, Supplement 2 Parameter Determination* Science (2002) Vol 298 page 1241-43.

6 Appendix

Attached are model files NFkB.c and NFkB.dat to encourage further use in MUSCOD-II.

```
/*
 * MUSCOD-II/BIOOPT/SRC/NFkB.c
 * (c) Achim Boltz, 2005
 */

#include <math.h>

#include "def_usrmod.h"
#include "def_ind.h"

#define NMOS 20
#define NP 41
#define NRC 0
#define NRCE 0

#define NXD 15
#define NXA 0
#define NU 0

#define NPR 0
#define NRD_S 0
#define NRDE_S 0

static double messwerte0[19]={0.0001,-1,-1,0.7974,1,
0.514,-1,-1,-1,-1,-1,-1,-1,-1,-1,-1,-1,-1,-1,-1};
static double messwerte1[19]={0.8983,0.6564,-1,1,
0.9145,0.6759,0.6377,-1,-1,-1,-1,-1,-1,-1,-1,-1,-1,-1,-1};
static double messwerte2[19]={0.1741,1,-1,0.2804,0.1542,
```

```

0.1652,0.1625,-1,-1,-1,-1,-1,-1,-1,-1,-1,-1,-1,-1,-1};
static double messwerte3[19]={0.2823,0.0488,0.0449,0.0964,
0.6716,1,0.6661,-1,0.2986,-1,-1,-1,-1,-1,-1,-1,-1,-1,-1};
static double messwerte4[19]={0.4267,0.8326,0.7873,1,0.7102,
0.7183,0.7553,-1,0.6121,-1,-1,-1,-1,-1,-1,-1,-1,-1,-1};
static double messwerte5[19]={0.0473,-1,-1,0.6639,1,0.8963,
0.6032,0.7335,-1,-1,-1,-1,-1,-1,-1,-1,-1,-1,-1};

static double messA20def0[19]={-1,-1,-1,-1,-1,-1,-1,-1,-1,-1,
-1,0.7228,0.8704,-1,1,0.7179,0.6110,0.5767,-1,-1};
static double messA20def1[19]={-1,-1,-1,-1,-1,-1,-1,-1,-1,-1,
-1,0.2054,1,-1,0.3526,0.3482,0.4828,0.4502,-1,-1};
static double messA20def2[19]={-1,-1,-1,-1,-1,-1,-1,-1,-1,-1,
-1,1,0.1615,0.1319,0.1784,0.1049,0.2360,0.2056,-1,0.1469};
static double messA20def3[19]={-1,-1,-1,-1,-1,-1,-1,-1,-1,-1,
-1,0.5669,0.7850,0.9446,0.9306,1,0.9768,0.9608,-1,0.9209};
static double messA20def4[19]={-1,-1,-1,-1,-1,-1,-1,-1,-1,-1,
-1,0.0840,-1,-1,0.6368,0.8050,0.9065,0.8744,1,-1};

static double xsca[15]={1.0e-0,1.0e-0,1.0e-0,1.0e-0,1.0e-0,1.0e-0,
1.0e-0,1.0e-0,1.0e-0,1.0e-0,1.0e-0,1.0e-0,1.0e-0,1.0e-0,1.0e-0};

static void rhsfcn(double *t, double *xd, double *xa, double *u,
double *p, double *rhs, double *rwh, long *iwh, long *info, double TR)
{
double kv, kprod, kdeg, a1, a2, a3, c1, c2, c3, c4, c5, c1a, c2a, c3a, c4a,
c5a, c6a, c1c, c2c, c3c, e1a, e2a, i1, i1a, k1, k2, k3, t1, t2, y1, y2, y3,
y4, y5, y6, y7, y8, y9, y10, y11, y12, y13, y14, y15, dy1, dy2, dy3, dy4,
dy5, dy6, dy7, dy8, dy9, dy10, dy11, dy12, dy13, dy14, dy15;

int i=0;
extern double xsca[15];

/* Umbenennung der Zustaeude */
for (i=0;i<15;i++){
xd[i]=xd[i]*xsca[i];
}

```

```
y1=xd[0];
y2=xd[1];
y3=xd[2];
y4=xd[3];
y5=xd[4];
y6=xd[5];
y7=xd[6];
y8=xd[7];
y9=xd[8];
y10=xd[9];
y11=xd[10];
y12=xd[11];
y13=xd[12];
y14=xd[13];
y15=xd[14];
```

```
kv=p[0];
kprod=p[1]*1e-6;
kdeg=p[2]*1e-5;
a1=p[3]*1e-2;
a2=p[4]*1e-2;
a3=p[5]*1e-1;
c1=p[6]*1e-8;
c2=p[7]*1e-7;
c3=p[8]*1e-5;
c4=p[9]*1e-2;
c5=p[10]*1e-5;
c1a=p[11]*1e-8;
c2a=p[12]*1e-7;
c3a=p[13]*1e-5;
c4a=p[14]*1e-2;
c5a=p[15]*1e-5;
c6a=p[16]*1e-6;
c1c=p[17]*1e-8;
c2c=p[18]*1e-7;
c3c=p[19]*1e-5;
e1a=p[20]*1e-5;
```

```

e2a=p[21]*1e-3;
i1=p[22]*1e-4;
i1a=p[23]*1e-4;
k1=p[24]*1e-4;
k2=p[25]*1e-2;
k3=p[26]*1e-4;
t1=p[27]*1e-2;
t2=p[28]*1e-2;

```

```

/*%%%%%%%%%%%%%%%%%%%%%%%%%%%%%%%%%%%%%%%%%%%%%%%%%%%%%%%%%%%%%%%%%%%%%%%%%%%%%%
%      xd[0] = y(1)   IKKn   neutral      %
%      xd[1] = y(2)   IKKa   active       %
%      xd[2] = y(3)   IKKi   inactive     %
%      xd[3] = y(4)   (IKKa|IkBa)        %
%      xd[4] = y(5)   (IKKa|IkBa|NFkB)   %
%      xd[5] = y(6)   NFkB                %
%      xd[6] = y(7)   NFkBn               %
%      xd[7] = y(8)   A20                 %
%      xd[8] = y(9)   A20t                %
%      xd[9] = y(10)  IkBa                %
%      xd[10] = y(11) IkBan               %
%      xd[11] = y(12) IkBat               %
%      xd[12] = y(13) (IkBa|NFkB) cytoplasmic %
%      xd[13] = y(14) (IkBan|NFkBn) nuclear %
%      xd[14] = y(15) Control early gene   %
%%%%%%%%%%%%%%%%%%%%%%%%%%%%%%%%%%%%%%%%%%%%%%%%%%%%%%%%%%%%%%%%%%%%%%%%%%%%%%*/

```

```

/* Gleichungen */

```

```

dy1=kprod-kdeg*y1-TR*k1*y1;
dy2=TR*k1*y1-k3*y2-TR*k2*y2*y8-kdeg*y2-a2*y2*y10+t1*y4-a3*y2*y13+t2*y5;
dy3=k3*y2+TR*k2*y2*y8-kdeg*y3;
dy4=a2*y2*y10-t1*y4;
dy5=a3*y2*y13-t2*y5;
dy6=c6a*y13-a1*y6*y10+t2*y5-i1*y6;
dy7=i1*kv*y6-a1*y11*y7;
dy8=c4*y9-c5*y8;
dy9=c2+c1*y7-c3*y9;
dy10=-a2*y2*y10-a1*y10*y6+c4a*y12-c5a*y10-i1a*y10+e1a*y11;

```

```

dy11=-a1*y11*y7+i1a*kv*y10-e1a*kv*y11;
dy12=c2a+c1a*y7-c3a*y12;
dy13=a1*y10*y6-c6a*y13-a3*y2*y13+e2a*y14;
dy14=a1*y11*y7-e2a*kv*y14;
dy15=c2c+c1c*y7-c3c*y15;

/* Output */
rhs[0]=dy1;
rhs[1]=dy2;
rhs[2]=dy3;
rhs[3]=dy4;
rhs[4]=dy5;
rhs[5]=dy6;
rhs[6]=dy7;
rhs[7]=dy8;
rhs[8]=dy9;
rhs[9]=dy10;
rhs[10]=dy11;
rhs[11]=dy12;
rhs[12]=dy13;
rhs[13]=dy14;
rhs[14]=dy15;

for (i=0;i<15;i++){
rhs[i]=rhs[i]*3600/xsca[i];
}
};

static void ffcn0(double *t, double *xd, double *xa, double *u,
double *p, double *rhs, double *rwh, long *iwh, long *info)
{
rhsfcn(t,xd,xa,u,p,rhs,rwh,iwh,info, 0);
};

static void ffcn1(double *t, double *xd, double *xa, double *u,
double *p, double *rhs, double *rwh, long *iwh, long *info)
{
rhsfcn(t,xd,xa,u,p,rhs,rwh,iwh,info, 1);
};

```

```

};

static void ffcn2(double *t, double *xd, double *xa, double *u,
double *p, double *rhs, double *rwh, long *iwh, long *info)
{
rhsfcn(t,xd,xa,u,p,rhs,rwh,iwh,info, 0);
rhs[7]=-xd[7]/5; // ab Stufe 10 sollen A20&A20t 0 sein,
// rhs dieser Zustnde wird im Nachhinein verndert
rhs[8]=-xd[8]/5;

};

static void ffcn3(double *t, double *xd, double *xa, double *u,
double *p, double *rhs, double *rwh, long *iwh, long *info)
{
rhsfcn(t,xd,xa,u,p,rhs,rwh,iwh,info, 1);
rhs[7]=-xd[7]/5;
rhs[8]=-xd[8]/5;
};

static void lsqfcn(
double *ts, /* physical time (I) */
double *sd, /* differential state vector (I) */
double *sa, /* algebraic state vector (I) */
double *u, /* control vector (I) */
double *p, /* global model parameter vector (I) */
double *pr, /* local i.p.c. parameter vector (I) */
double *res, /* i.p.c. residual (0) */
long *dpnd, /* argument dependency code (I/0) */
long *info /* error code (0) */
)
/*
* decoupled or coupled interior point constraint (i.p.c.) residual
*/
{
int i=0;
long mstage;

```

```

double m1, m2, m3, m4, m5, m6, m7, m8, m9, m10, m11;

m1=p[29];
m2=p[30];
m3=p[31];
m4=p[32];
m5=p[33];
m6=p[34];
m7=p[35];
m8=p[36];
m9=p[37];
m10=p[38];
m11=p[39];

if (*dpnd) {
    *dpnd = RFCN_DPND(*ts, *sd, *sa, *u, *p, *pr);
    return;
}

get_cimos(&mstage); //---->speichert die stagenummer in der "long" variable mstage
for (i=0;i<11;i++){res[i]=0;}

if (mstage!=0)
{
if (messwerte0[mstage-1]!=-1){
res[0]=sd[8]/m1-messwerte0[mstage-1];
// sd/m-mess entspricht (sd-mess*m)/m <- als Gewicht
};

if (messwerte1[mstage-1]!=-1){
res[1]=(sd[0]+sd[1]+sd[2])/m2-messwerte1[mstage-1];
};

if (messwerte2[mstage-1]!=-1){
res[2]=sd[1]/m3-messwerte2[mstage-1];
};
}

```

```

if (messwerte3[mstage-1] != -1){
res[3]=(sd[3]+sd[4]+sd[9]+sd[12])/m4-messwerte3[mstage-1];
};

if (messwerte4[mstage-1] != -1){
res[4]=sd[6]/m5-messwerte4[mstage-1];
};

if (messwerte5[mstage-1] != -1){
res[5]=sd[11]/m6-messwerte5[mstage-1];
};

if (messA20def0[mstage-1] != -1){
res[6]=(sd[0]+sd[1]+sd[2])/m7-messA20def0[mstage-1];
};

if (messA20def1[mstage-1] != -1){
res[7]=sd[1]/m8-messA20def1[mstage-1];
};

if (messA20def2[mstage-1] != -1){
res[8]=(sd[3]+sd[4]+sd[9]+sd[12])/m9-messA20def2[mstage-1];
};

if (messA20def3[mstage-1] != -1){
res[9]=sd[6]/m10-messA20def3[mstage-1];
};

if (messA20def4[mstage-1] != -1){
res[10]=sd[11]/m11-messA20def4[mstage-1];
};
};

static void lsqfcn1(
double *ts, /* physical time (I) */
double *sd, /* differential state vector (I) */

```

```

double *sa, /* algebraic state vector (I) */
double *u, /* control vector (I) */
double *p, /* global model parameter vector (I) */
double *pr, /* local i.p.c. parameter vector (I) */
double *res, /* i.p.c. residual (0) */
long *dpnd, /* argument dependency code (I/0) */
long *info /* error code (0) */
)
{
    int i;
    double w;
    w=p[40];
    if (*dpnd) {
        *dpnd = RFCN_DPND(*ts, *sd, *sa, *u, *p, *pr);
        return;
    }
    res[0 ]=(p[0] - 5);
    res[1 ]=p[1] - 25;
    res[2 ]=p[2] - 12.5;
    res[3 ]=p[3] - 50;
    res[4 ]=p[4] - 20;
    res[5 ]=p[5] - 10;
    res[6 ]=p[6] - 50;
    res[7 ]=p[7] - 0;
    res[8 ]=p[8] - 40;
    res[9 ]=p[9] - 50;
    res[10]=p[10] - 30;
    res[11]=p[11] - 50;
    res[12]=p[12] - 0;
    res[13]=p[13] - 40;
    res[14]=p[14] - 50;
    res[15]=p[15] - 10;
    res[16]=p[16] - 20;
    res[17]=p[17] - 50;
    res[18]=p[18] - 0;
    res[19]=p[19] - 40;
    res[20]=p[20] - 50;
    res[21]=p[21] - 10;

```

```

res[22]=p[22] - 25;
res[23]=p[23] - 10;
res[24]=p[24] - 25;
res[25]=p[25] - 10;
res[26]=p[26] - 15;
res[27]=p[27] - 10;
res[28]=p[28] - 10;
res[29]=p[29] - 1.8128138195410299E-04;
res[30]=p[30] - 2.5064559896630589E-01;
res[31]=p[31] - 7.3594759361470988E-02;
res[32]=p[32] - 1.0795282048348229E-01;
res[33]=p[33] - 2.5716898124625243E-01;
res[34]=p[34] - 1.6736725108767580E-04;
res[35]=p[35] - 2.6602679751446251E-01;
res[36]=p[36] - 8.2737528790542664E-02;
res[37]=p[37] - 7.8206334116788526E-02;
res[38]=p[38] - 2.6554325741738211E-01;
res[39]=p[39] - 2.9478697184882294E-04;

for (i=0;i<40;i++){
res[i]=res[i]*w;
}

};

void def_model(void)
{
long i;
def_mdims(NMOS, NP, NRC, NRCE);

def_msolver(1, def_DAESOL);

def_mstage(
0,
NXD, NXA, NU,
NULL, NULL,
0, 0, 0, NULL, ffcn0, NULL,
NULL, NULL,

```

```

    0
);

for (i=1;i<10;i++){
  def_mstage(
i,
NXD, NXA, NU,
NULL, NULL,
0, 0, 0, NULL, ffcn1, NULL,
NULL, NULL,
0
);
}

def_mstage(
  10,
  NXD, NXA, NU,
  NULL, NULL,
  0, 0, 0, NULL, ffcn2, NULL,
  NULL, NULL,
  0
);

for (i=11;i<20;i++){
  def_mstage(
i,
NXD, NXA, NU,
NULL, NULL,
0, 0, 0, NULL, ffcn3, NULL,
NULL, NULL,
0
);
}
def_lsq(0, "s",0 , 40, lsqfcn1);
for (i=1;i<20;i++){
  def_lsq(i, "s",0 , 11, lsqfcn);
}

```

```
}  
}
```

```
* MUSCOD-II/BIOOPT/DAT/NFkB.dat  
* (c) Achim Boltz 2005
```

```
* # of multiple shooting intervals on each model stage
```

```
nshoot
```

```
0: 3
```

```
1: 3
```

```
2: 3
```

```
3: 3
```

```
4: 3
```

```
5: 3
```

```
6: 3
```

```
7: 3
```

```
8: 3
```

```
9: 3
```

```
10: 3
```

```
11: 3
```

```
12: 3
```

```
13: 3
```

```
14: 3
```

```
15: 3
```

```
16: 3
```

```
17: 3
```

```
18: 3
```

```
19: 3
```

```
* model stage duration start values, scale factors, and bounds
```

```
h
```

```
0: 101
```

```
1: 0.166666
```

```
2: 0.166666
```

```
3: 0.166666
```

```
4: 0.5
```

```
5: 0.5
```

6: 0.5
7: 0.5
8: 0.5
9: 4
10: 101
11: 0.166666
12: 0.166666
13: 0.166666
14: 0.5
15: 0.5
16: 0.5
17: 0.5
18: 0.5
19: 4

plot_first
1

plot_last
9

h_sca
0: 1.0
1: 1.0
2: 1.0
3: 1.0
4: 1.0
5: 1.0
6: 1.0
7: 1.0
8: 1.0
9: 1.0
10: 1
11: 1
12: 1
13: 1
14: 1
15: 1

16: 1
17: 1
18: 1
19: 1

h_min

0: 0
1: 0
2: 0
3: 0
4: 0
5: 0
6: 0
7: 0
8: 0
9: 0
10: 0
11: 0
12: 0
13: 0
14: 0
15: 0
16: 0
17: 0
18: 0
19: 0

h_max

0: 200
1: 200
2: 200
3: 200
4: 200
5: 200
6: 200
7: 200
8: 200

9: 200
10: 200
11: 200
12: 200
13: 200
14: 200
15: 200
16: 200
17: 200
18: 200
19: 200

h_fix

0: 1
1: 1
2: 1
3: 1
4: 1
5: 1
6: 1
7: 1
8: 1
9: 1
10: 1
11: 1
12: 1
13: 1
14: 1
15: 1
16: 1
17: 1
18: 1
19: 1

h_name

0: !
1: !
2: !

3: !
4: !
5: !
6: !
7: !
8: !
9: !
10: !
11: !
12: !
13: !
14: !
15: !
16: !
17: !
18: !
19: !

* specification mode for differential state variable start values
s_spec

2

* differential state start values, scale factors, and bounds

sd(0,0)

0: 0

1: 0

2: 0

3: 0

4: 0

5: 0

6: 0

7: 0

8: 0

9: 0

10: 0

11: 0

12: 0.06

13: 0

14: 0

sd_fix(0,0)

0: 1
1: 1
2: 1
3: 1
4: 1
5: 1
6: 1
7: 1
8: 1
9: 1
10: 1
11: 1
12: 1
13: 1
14: 1

sd_sca(*,*)

0: 1
1: 1
2: 1
3: 1
4: 1
5: 1
6: 1
7: 1
8: 1
9: 1
10: 1
11: 1
12: 1
13: 1
14: 1

sd_min(*,*)

0: -100000
1: -100000
2: -100000
3: -100000
4: -100000
5: -100000
6: -100000
7: -100000
8: -100000
9: -100000
10: -100000
11: -100000
12: -100000
13: -100000
14: -100000

sd_max(*,*)

0: 10000000
1: 10000000
2: 10000000
3: 10000000
4: 10000000
5: 10000000
6: 10000000
7: 10000000
8: 10000000
9: 10000000
10: 10000000
11: 10000000
12: 10000000
13: 10000000000
14: 10000000000

xd_name

0: >A IKKn
1: B IKKa
2: C IKKi

3: D IKKa:IkBa
4: E IKKa:IkBa:NFkB
5: F NFkB
6: G NFkBn
7: H A20
8: I A20t
9: J IkBa
10: K IkBan
11: L IkBat
12: M IkBa:NFkB
13: N IkBan:NFkBn
14: O control gen mRNA

xd_unit

0: M
1: M
2: M
3: M
4: M
5: M
6: M
7: M
8: M
9: M
10: M
11: M
12: M
13: M
14: M

*****Lipniacki's Version of Parameters*****

p

0: 5
1: 25
2: 12.5
3: 50
4: 20
5: 10

6: 50
7: 0
8: 40
9: 50
10: 30
11: 50
12: 0
13: 40
14: 50
15: 10
16: 20
17: 50
18: 0
19: 40
20: 50
21: 10
22: 25
23: 10
24: 25
25: 10
26: 15
27: 10
28: 10
29: 1.8128138195410299E-04
30: 2.5064559896630589E-01
31: 7.3594759361470988E-02
32: 1.0795282048348229E-01
33: 2.5716898124625243E-01
34: 1.6736725108767580E-04
35: 2.6602679751446251E-01
36: 8.2737528790542664E-02
37: 7.8206334116788526E-02
38: 2.6554325741738211E-01
39: 2.9478697184882294E-04
40: 1.0e-2

p_fix

0: 0
1: 0
2: 0
3: 0
4: 0
5: 0
6: 0
7: 0
8: 0
9: 0
10: 0
11: 0
12: 0
13: 0
14: 0
15: 0
16: 0
17: 1 *\
18: 1 * cgen
19: 1 */
20: 0
21: 0
22: 0
23: 0
24: 0
25: 0
26: 0
27: 0
28: 0
29: 0 *ab hier die m's
30: 0
31: 0
32: 0
33: 0
34: 0
35: 0
36: 0
37: 0

38: 0
39: 0
40: 1

p_name
0: !kv
1: !kprod
2: !kdeg
3: !a1
4: !a2
5: !a3
6: !c1
7: !c2
8: !c3
9: !c4
10: !c5
11: !c1a
12: !c2a
13: !c3a
14: !c4a
15: !c5a
16: !c6a
17: !c1c
18: !c2c
19: !c3c
20: !e1a
21: !e2a
22: !i1
23: !i1a
24: !k1
25: !k2
26: !k3
27: !t1
28: !t2
29: m1
30: m2
31: m3

32: m4
33: m5
34: m6
35: m7
36: m8
37: m9
38: m10
39: m11
40: !Weight

p_unit

0:
1: E-6M/s
2: E-5/s
3: E-2M/s
4: E-2M/s
5: E-1M/s
6: E-8/s
7: E-9M/s
8: E-5/s
9: E-2/s
10: E-5/s
11: E-8/s
12: E-9M/s
13: E-5/s
14: E-2/s
15: E-5/s
16: E-6/s
17: E-8/s
18: E-9M/s
19: E-5/s
20: E-5/s
21: E-3/s
22: E-4/s
23: E-4/s
24: E-4/s
25: E-2/s

26: E-4/s
27: E-2/s
28: E-2/s
29: M
30: M
31: M
32: M
33: M
34: M
35: M
36: M
37: M
38: M
39: M
40:

p_sca

0: 1
1: 1
2: 1
3: 1
4: 1
5: 1
6: 1
7: 1
8: 1
9: 1
10: 1
11: 1
12: 1
13: 1
14: 1
15: 1
16: 1
17: 1
18: 1
19: 1
20: 1

21: 1
22: 1
23: 1
24: 1
25: 1
26: 1
27: 1
28: 1
29: 1
30: 1
31: 1
32: 1
33: 1
34: 1
35: 1
36: 1
37: 1
38: 1
39: 1
40: 1

p_min
0: 1
1: 0
2: 0
3: 40
4: 0
5: 0
6: 0
7: 0
8: 0
9: 0
10: 0
11: 0
12: 0
13: 30
14: 0
15: 1

16: 10
17: 0
18: 0
19: 0
20: 10
21: 0.01
22: 1
23: 1
24: 0
25: 0
26: 0
27: 0
28: 0
29: 0.000001
30: 0.000001
31: 0.000001
32: 0.000001
33: 0.000001
34: 0.000001
35: 0.000001
36: 0.000001
37: 0.000001
38: 0.000001
39: 0.000001
40: 0

p_max

0: 6
1: 1000
2: 1000
3: 60
4: 1000
5: 1000
6: 1000
7: 1.5e-9
8: 1000
9: 1000
10: 1000

11: 1000
12: 1.5e-9
13: 50
14: 1000
15: 20
16: 30
17: 1000
18: 1000
19: 1000
20: 9000
21: 9
22: 900
23: 900
24: 1000
25: 1000
26: 1000
27: 1000
28: 1000
29: 1000
30: 1000
31: 1000
32: 1000
33: 1000
34: 1000
35: 1000
36: 1000
37: 1000
38: 1000
39: 1000
40: 1000

of_sca
1

of_min
0

of_max

10

of_name

!least squares

nhist

20

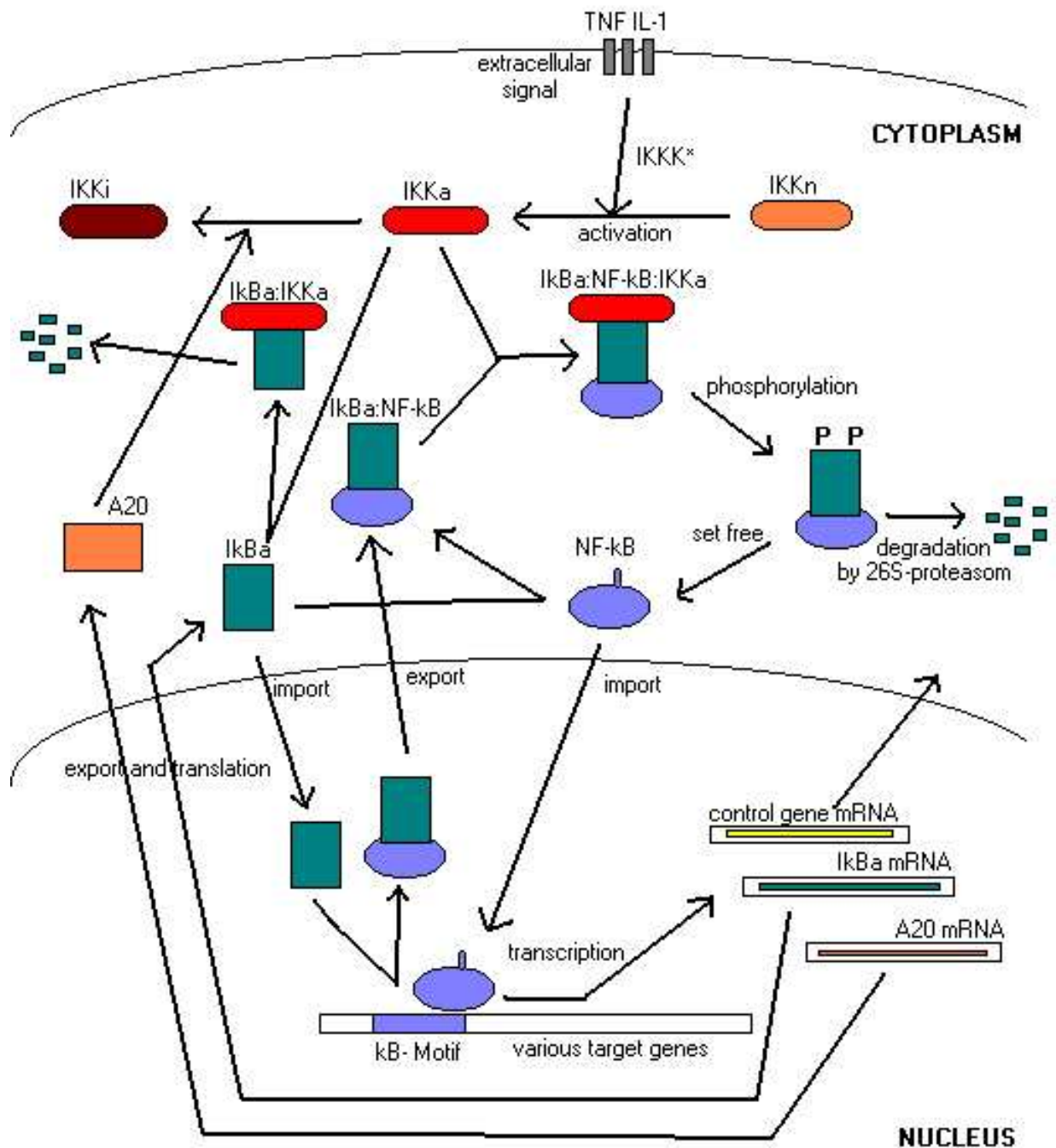


Figure 1: schematic overview of the regulatory model. Upon TNF or IL-1 stimulation, IKKK activates IKKn into its active form IKKa. Active IKKa forms complexes with $I\kappa B\alpha$ and $I\kappa B\alpha:NF-\kappa B$ and phosphorylates it which leads to fast degradation. Liberated $NF-\kappa B$ enters the nucleus where it binds to κB motifs in A20, $I\kappa B\alpha$ or other gene promoters. The newly synthesized $I\kappa B\alpha$ enters the nucleus and leads $NF-\kappa B$ again to cytoplasm, while newly synthesized A20 triggers transformation of IKKa into inactive IKKi.

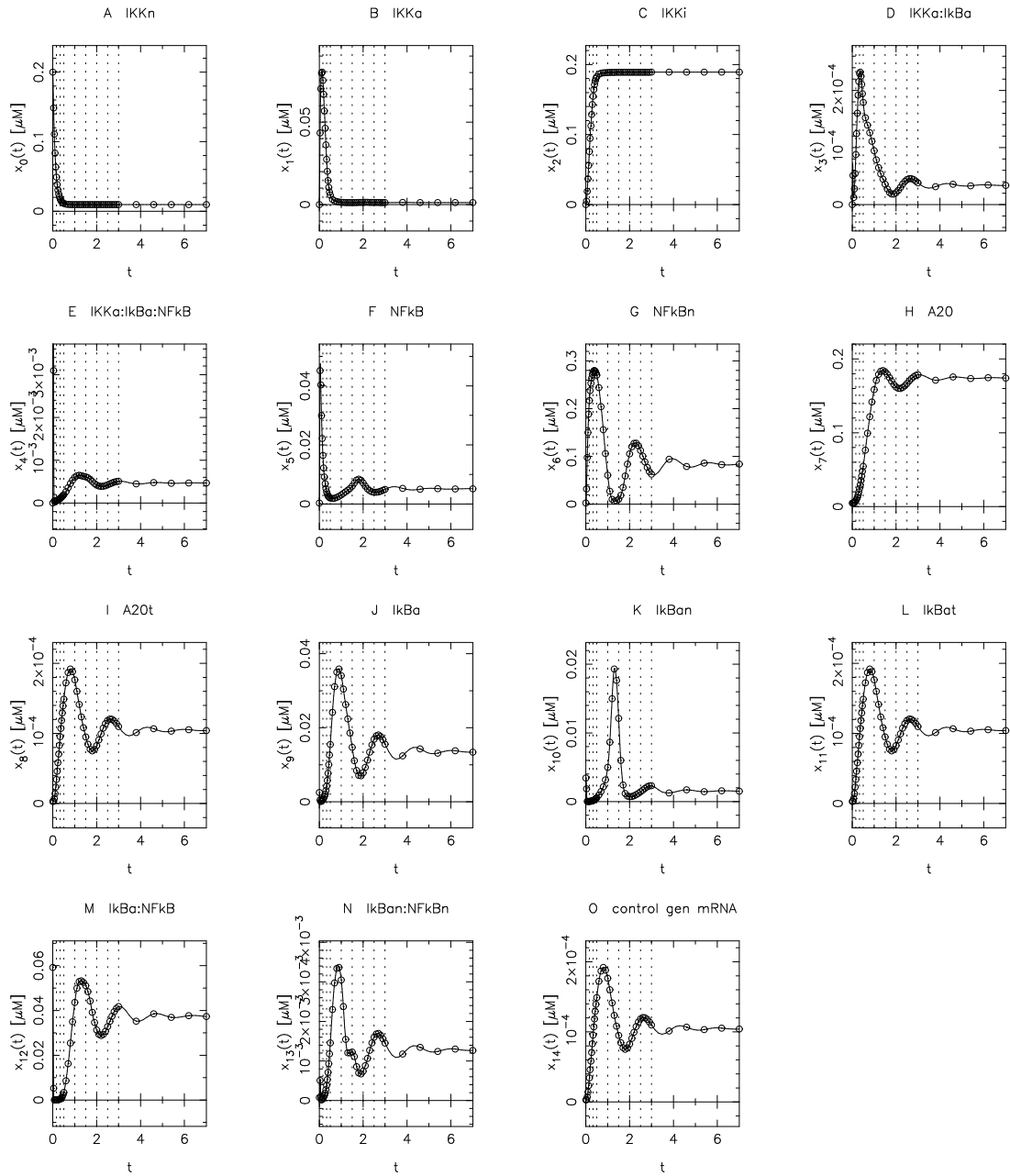


Figure 2: Numerical solution for model of wildtype cells based on parameters estimated by Lipniacki et al. Concentrations are given in μM and time is in hours. Recognizable lines within the graphs indicate the points in time in which experimental data is available to be compared to model predictions.

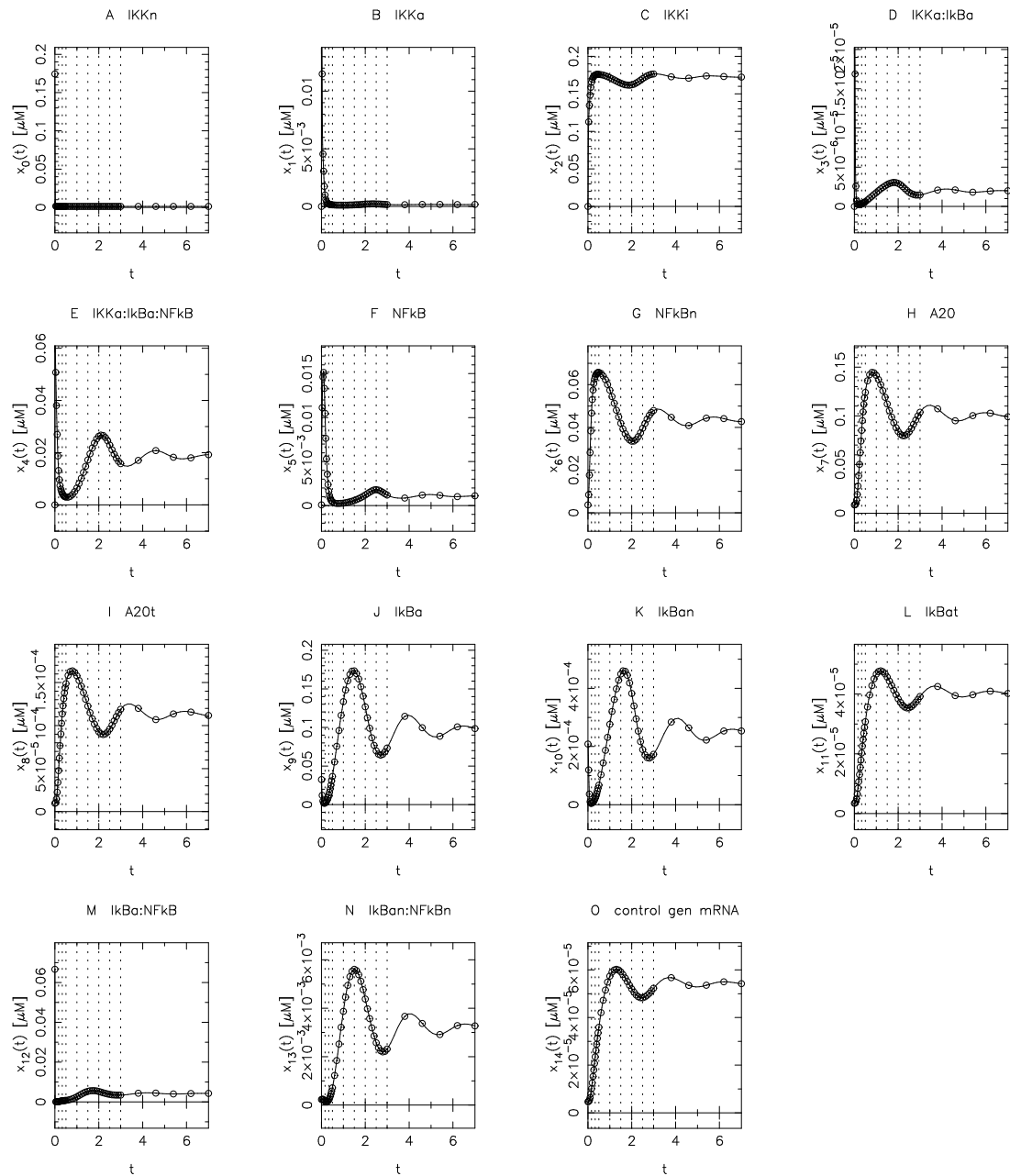


Figure 3: Numerical solution for model of wildtype cells. Concentrations are given in μM and time is in hours. Recognizable lines within the graphs indicate the points in time in which experimental data is available to be compared to model predictions.

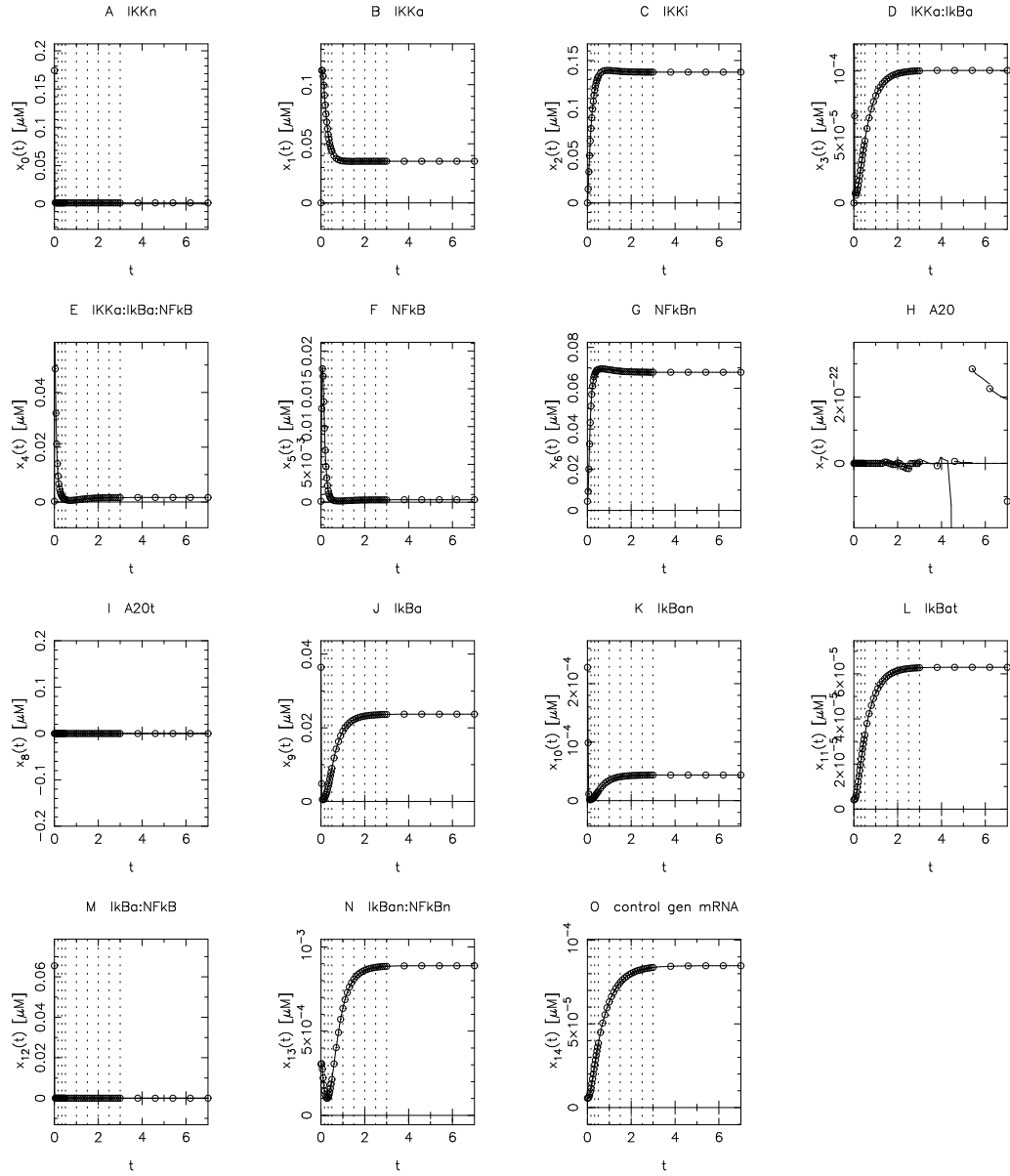


Figure 4: Numerical solution for model of A20 deficient cells. Concentrations are given in μM and time is in hours. Recognizable lines within the graphs indicate the points in time in which experimental data is available to be compared to model predictions. Values for A20 protein in panel H at 5 hours different from 0 are an artefact of simulation and can be considered as 0.

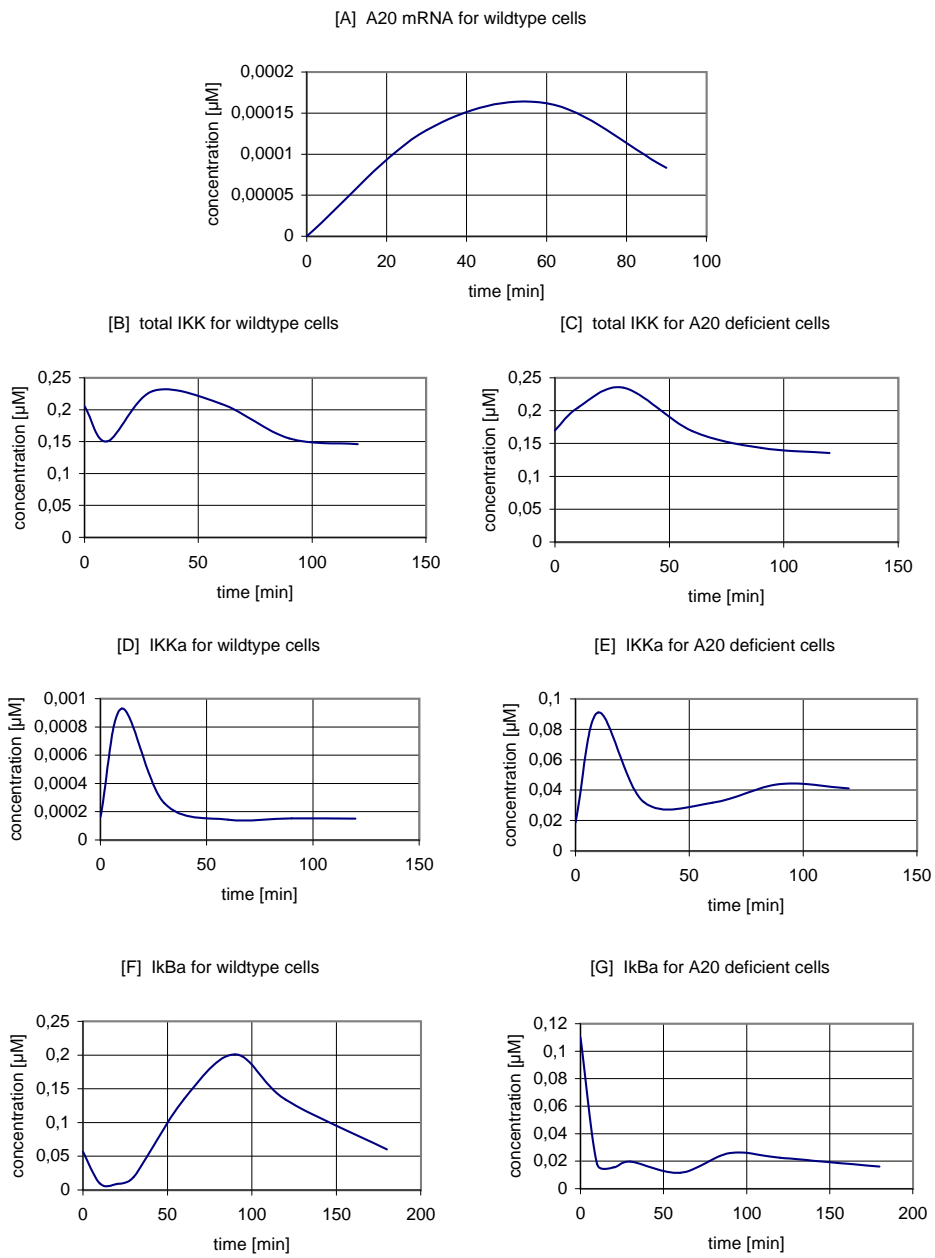


Figure 5: Graphs for measurements over time, already multiplied by estimated normalization factors. Panels [A] to [G]. Concentrations are given in μM , time in minutes.

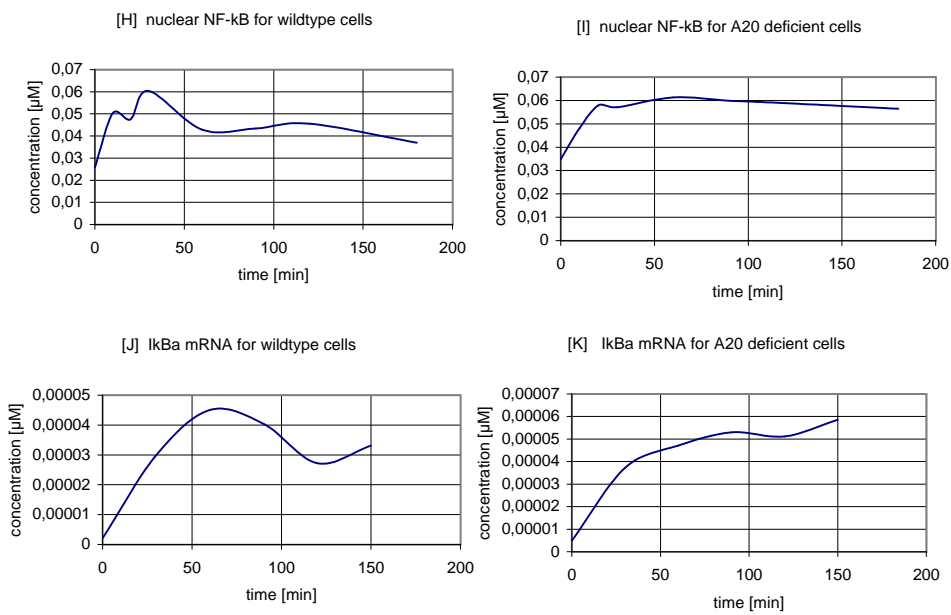


Figure 6: Graphs for measurements over time, already multiplied by estimated normalization factors. Panels [H] to [K]. Concentrations are given in μM , time in minutes.